Research on recognition of human lying posture based on Kinect sensor

Qi Wang
Changchun University of Science and Technology https://orcid.org/0000-0001-6940-6533
Xianyu Meng (mxy800809@126.com)
Changchun University of Science and Technology
Cong Li
AVIC Aerodynaiviics Research Institute,Harbin,Heilongjiang,China
Hongsheng Liu
Changchun University of Science and Technology
Xiquan Yu
Changchun University of Science and Technology

Research

Keywords: intelligent nursing bed, recognition of lying posture, Kinect sensor, bone data, neural network.

Posted Date: April 26th, 2021

DOI: https://doi.org/10.21203/rs.3.rs-390860/v1

Title：

Research on recognition of human lying posture based on Kinect sensor

Qi Wang: Changchun University of Science and Technology
Xianyu Meng: Changchun University of Science and Technology
Cong Li: AVIC Aerodynaiviics Research Institute, Harbin, Heilongjiang, China
Hongsheng Liu: Changchun University of Science and Technology
Xiquan Yu: Changchun University of Science and Technology
Correspondence：mxy800809@126.com

Abstract: As a high-tech intelligent product, the intelligent nursing bed largely meets the needs of the disabled for self-care, and saves a lot of manpower and material resources. In order to improve the safety and reliability of the intelligent nursing bed and ensure the safety of the user, this paper adds the recognition of the human body's lying posture as a part of the movement signal of the nursing bed. The Kinect sensor is used to track human bones, record human bone data, and preprocess human bone data. Use the pattern recognition toolbox in Matlab to classify the processed data to realize the recognition of the human body's lying posture. The average recognition rate of the five postures is 98.1%. The results show that the model used in this experiment has a high degree of recognition and can greatly improve the safety and reliability of the intelligent nursing bed.

Key words: intelligent nursing bed; recognition of lying posture; Kinect sensor; bone data; neural network.

1 Introduction

The nursing of long-term bedridden patients is an inevitable and very labor-intensive task for families and nursing institutions and hospitals, especially for critically ill patients who have lost part of their body functions. It's getting more and more prominent. Therefore, people are focusing on smart nursing beds to solve the basic nursing problems of the elderly who cannot take care of themselves, the patients with mobility problems and the disabled due to diseases, and reduce the nursing pressure of medical staff and patients' families. As a medical auxiliary device, it has basic functions such as raising the back, bending the legs, and turning left and right. However, the automatic control of most nursing beds is controlled by a fixed time, and there are certain hidden safety hazards. May cause more harm to the user. Therefore, improving the safety and reliability of nursing beds is particularly important for the development of intelligent nursing beds.

Aiming at the hidden safety hazards of the intelligent nursing bed, this paper designs a human bone data preprocessing algorithm combined with the recognition system model of the pattern recognition toolbox in Matlab according to the bone data of the human body. The system can recognize the lying posture of the human body, and output the signal as a part of the motion signal of the intelligent nursing bed, which greatly improves the safety and reliability of the intelligent nursing bed.

2 Method

2.1 Recognition model design

The work flow of the human body gesture recognition model designed in this paper is shown in Figure 1. The work flow is as follows: first collect the subject's human bone data information through the Kinect sensor, and then use the designed algorithm to select and compare the bone feature points. The coordinates of the bone points are transformed and the joint angle features are calculated. Finally, the Matlab pattern recognition toolbox is used to identify the processed features to determine the current posture of the human body.

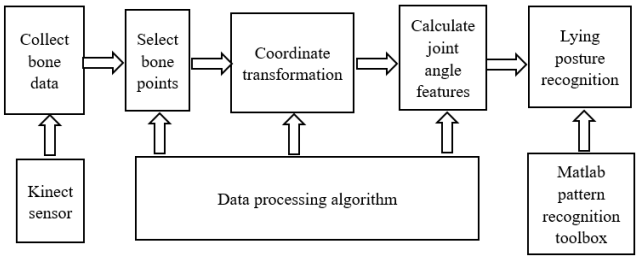

Fig.1 Model design flow chart

2.2 Data collection

2.2.1 Acquisition equipment

The Kinect sensor includes a color camera, infrared transmitter and receiver, and four microphone arrays. In Kinect sensor, the RGB camera captures a color image with a resolution of 1920×1080 pixels at 30 frames per second, while an infrared camera also obtains infrared data and a depth map with a resolution of 512×424 pixels in real time at 30 frames per second. Kinect sensor has a field of view of 70 degrees horizontally and 60 degrees vertically, and the measured depth distance is 0.5 m-4.5 m. It can obtain information on 25 joint points of the human body, and can detect 6 people

at the same time. The user can also adjust the motor base The direction and angle to obtain the ideal image data.

2.2.2 Data collection

In order to obtain the data set required for training the neural network, this paper collected the human bones of 10 normal subjects (3 women and 7 men, aged between 25-60 years and height between 1.55-1.90 m) data information. When collecting data in this experiment, the subjects lay on the intelligent nursing bed and presented five postures: lying flat, raising the back, bent legs, and lying on the left and right sides. The Kinect sensor collects the human bone data information, and each posture is maintained 10 seconds. As shown in Figure 2. Part of the output data after the collection is completed is shown in Figure 3.

Fig.2 Human posture diagram

	x	y	z	x	y	z	x	y	z	x	y	z
Head	0.360343	0.433998	2.03399	0.362751	0.438181	2.03631	0.375324	0.448888	2.04386	0.375152	0.447817	2.04321
SpineShoulder	0.408351	0.285034	2.12404	0.409023	0.286061	2.1257	0.412423	0.288695	2.12954	0.411965	0.287238	2.1291
ShoulderLeft	0.26719	0.286823	2.24062	0.267294	0.293513	2.24344	0.268019	0.303929	2.25353	0.266748	0.302422	2.25196
ShoulderRight	0.531666	0.254488	2.07156	0.531742	0.251968	2.07092	0.534492	0.252397	2.07339	0.53488	0.253005	2.07396
SpineBase	0.385986	-0.13314	2.27621	0.395351	-0.13387	2.28492	0.384778	-0.1446	2.27178	0.378263	-0.1425	2.26378
HipLeft	0.448764	-0.13404	2.21755	0.458683	-0.13517	2.22209	0.439829	-0.15056	2.19987	0.433281	-0.14674	2.19249
HipRight	0.312565	-0.12885	2.27255	0.321977	-0.12869	2.2859	0.320698	-0.13466	2.28333	0.312511	-0.13522	2.27294
KneeLeft	0.174688	-0.21039	1.88368	0.185871	-0.20948	1.88677	0.252897	-0.19627	1.92797	0.218786	-0.18767	1.94277
KneeRight	-0.03258	-0.1958	2.01741	-0.00913	-0.20472	2.01403	0.011935	-0.14156	2.03395	0.057487	-0.1647	2.06951
AnkleLeft	0.019755	-0.43802	1.76122	0.002133	-0.40481	1.74806	0.052066	-0.39997	1.75648	0.063298	-0.38166	1.76744
AnkleRight	-0.10248	-0.40862	1.63718	-0.08301	-0.41396	1.66578	-0.06052	-0.37796	1.70966	-0.03659	-0.37032	1.7301

Fig.3 Part of the collected data diagram

2.3 Data processing

2.3.1 Selection of bone points

By using the Kinect sensor and the corresponding development software, the spatial coordinates (x, y, z) of the standardized bone joints of 25 human bodies can be obtained. However, since some of the joint points have no effect on gesture recognition, based on the reliability of the purpose of this research and the consideration of recognition speed, this paper screens the number of bone joints and reduces the number of bone joint points from 25 to 11. As shown in Figure 5, the selected 11 joint points are: head(1),spine shoulder(2),shoulder left(3),shoulder right(4),spine base(5),hip

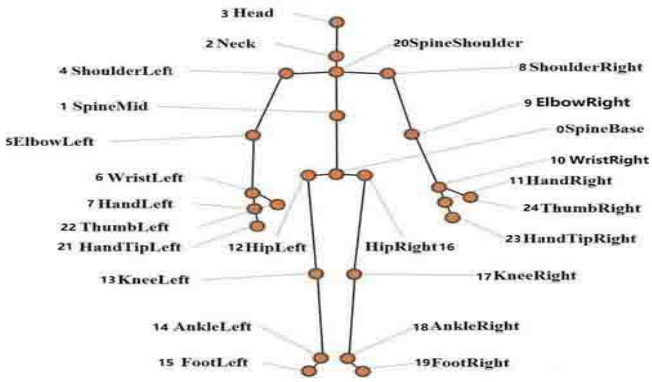

Fig. 4 25 standardized bone joint points

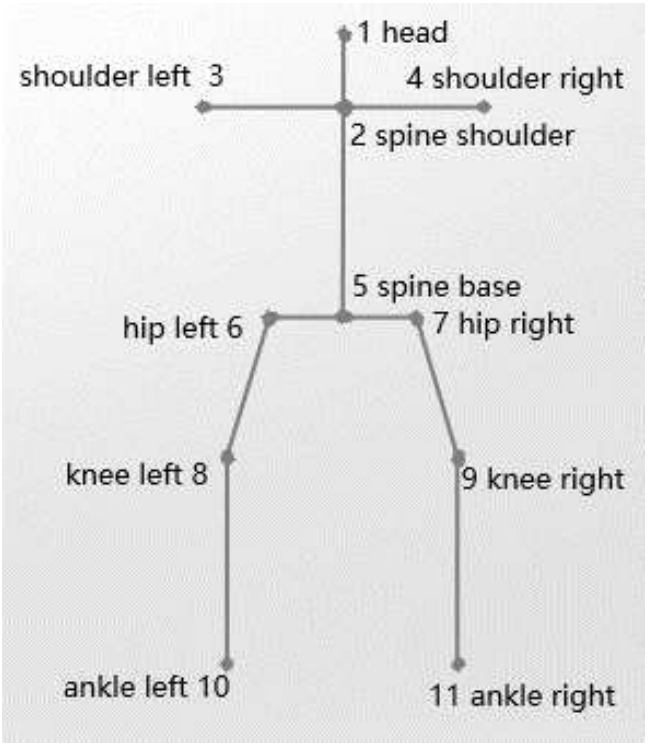

Fig. 5 Coordinate diagram of 11 joint points

left(6),hip right(7),knee left(8),knee right(9),ankle left(10),ankle right(11).

2.3.2 Coordinate transformation

In order to determine the position of the subjects on the intelligent nursing bed, coordinate transformation of the 11 selected bone joint coordinates is needed to transform them into the absolute reference system (x, y, z) with the intelligent nursing bed as the reference. According to the imaging theory [2], the world coordinate system $o_{w-x_w y_w z_w}$ can be converted to the imaging coordinate system o_{i-xyz} through $o_i = Ro_w + T$, where T is the transition matrix and R is the rotation matrix. In Kinect sensor, the coordinate transformation model can be represented by Figure 6.

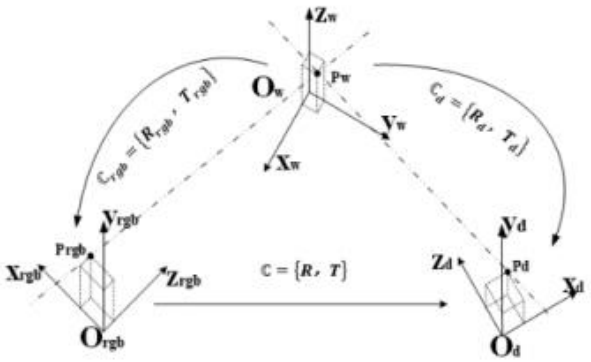

Fig. 6 Coordinate transformation model

Converting the world coordinate system to the depth system and the RGB system can use equation (1) and equation (2).

$$o_{d-x_d y_d z_d} = R_d o_{w-x_w y_w z_w} + T_d \quad (1)$$

$$o_{rgb-x_{rgb} y_{rgb} z_{rgb}} = R_{rgb} o_{w-x_w y_w z_w} + T_{rgb} \quad (2)$$

In the imaging system, the RGB image coordinate system $[u_{rgb}, v_{rgb}, 1]^T$ can be described by equation (3).

$$\begin{bmatrix} u_{rgb} \\ v_{rgb} \\ 1 \end{bmatrix} = \frac{1}{z_{rgb}} H_{rgb} \begin{bmatrix} x_{rgb} \\ y_{rgb} \\ z_{rgb} \end{bmatrix} \quad (3)$$

The depth imaging system can be described by equation (4).

$$\begin{bmatrix} u_d \\ v_d \\ 1 \end{bmatrix} = \frac{1}{z_d} H_d \begin{bmatrix} x_d \\ y_d \\ z_d \end{bmatrix} \quad (4)$$

Among them, H_{rgb} and H_d are the original parameters of the sensor. Through the above four formulas, the transformation from the form $[u_{rgb}, v_{rgb}, 1]^T$ to $[u_d, v_d, 1]^T$.Since the distance between the color camera and the depth camera of the Kinect sensor is very close, it can be assumed that $z_d \approx z_{rgb}$, so:

$$\begin{bmatrix} u_d \\ v_d \\ 1 \end{bmatrix} \approx H_d H_{rgb}^{-1} R_d R_{rgb}^{-1} \begin{bmatrix} u_{rgb} \\ v_{rgb} \\ 1 \end{bmatrix} + (T_d - R_d R_{rgb}^{-1} T_{rgb}) \quad (5)$$

Since the Kinect sensor is a standardized production equipment, solving the spatial mapping problem can be solved with the calibration parameters of Kinect sensor [1]. When solving the joint point $J(u_{rgb}, v_{rgb})$ in the color image, it can be used to obtain the depth image map $J(u_d, v_d)$ In the depth camera coordinate system, the depth value of P' is z_d.So far, the three-dimensional coordinates are based on the world The coordinate system $J(x_w, y_w, z_w)$ is obtained with respect to $J(u_{rgb}, v_{rgb})$ according to equations (2) and (3).

2.3.3 Node angle calculation

For any two joint points $P_i(x_i, y_i, z_i), P_j(x_j, y_j, z_j)$, the coordinates of the two joint points that need to be calculated can be obtained through the Kinect sensor. After the coordinate transformation, the formula (6) Calculate the direct distance between

two joint points. By continuing to process these distance features, the angle features between multiple joint points can be calculated.

$$d_{x,y,z} = \sqrt{(x_i - x_j)^2 + (y_i - y_j)^2 + (z_i - z_j)^2} \quad (6)$$

There are two main methods for calculating the angle characteristics of each group of joint points: the first is the three-point method, select the three human body joint points P_i, P_j and P_k that need to be calculated, and use the formula to calculate the relationship between the three joint points. The distances d_{ij}, d_{ik} and d_{jk}, and then the law of cosines (7) can be used to find the angle between each joint point.

$$\theta = \arccos\frac{a^2+b^2-c^2}{2ab} \quad (7)$$

The second method is the two-point method. Only two joint points P_i and P_j are used for each group of angles. Using P_i as the reference point, the connection between the two key points P_i and P_j and the reference point X are calculated by formula (8) The included angle of the axis.

$$\theta = \arccos\frac{x_j - x_i}{d_{ij}} \quad (8)$$

Through the above algorithm, processing the acquired data, a total of 10 joint angles can be obtained. Divide all the obtained joint angles by 180 degrees for normalization. From the above 10 joint angles, select the angle features needed for lying posture recognition during the experiment. As shown in Figure 7.

μ	α	β	γ	θ
90.02884	89.99931	91.37304	91.3349	90.35371
90.03275	89.98498	91.19414	91.79894	90.62031
90.03145	89.98374	91.25881	91.89519	90.60405
90.04135	89.9832	92.07469	91.25659	90.69108
90.04859	89.98171	91.7779	91.0944	90.69484
90.05041	89.98083	92.08256	92.56391	90.73667
90.05569	89.98037	91.9911	92.45289	90.74591
90.06052	89.98106	91.60578	91.9221	90.64708
90.06151	89.98185	91.17971	91.73123	90.61282
90.05996	89.9825	91.2544	91.94039	90.64067
90.05952	89.98235	91.27599	91.84926	90.63621
90.05818	89.98243	92.34753	91.96662	90.65368
90.05593	89.98263	92.48034	92.0082	90.62893
90.05602	89.98227	91.46762	92.24388	90.66315
90.05542	89.98271	91.33095	92.14475	90.64034
90.05567	89.98229	91.44611	92.3503	90.68249
90.05532	89.9819	92.1076	92.2835	90.6965
90.0545	89.98232	92.13376	92.43178	90.67318
90.05333	89.98237	92.18066	92.38876	90.6884
90.05278	89.98222	91.51078	92.7565	90.72148
90.05156	89.98221	91.46533	92.29784	90.67186
90.0514	89.98242	91.65727	92.20098	90.65457
90.05165	89.98277	91.53299	92.35413	90.66154
90.05296	89.98244	91.71136	92.50062	90.69881
90.05258	89.9829	91.55824	92.08239	90.64056
90.05273	89.98312	91.57112	92.15915	90.64271
90.05204	89.9832	91.33385	92.30261	90.65634
90.05158	89.98291	91.69997	92.38731	90.65542
90.05046	89.98501	91.43953	92.23699	90.69738

Fig. 7 Partial angle feature data map

2.4 Neural network recognition

2.4.1 Kinematics feature definition

This paper defines a set of characteristics that can not be affected by the body size of each subject to represent the kinematic characteristics of different human postures, that is, from the above 10 joint angles, 5 angles are selected As features for identification, they are: the angle μ between the head and the left shoulder, the angle α between the head and the right shoulder, the angle β between the thigh and the calf, and

the angle between the shoulder and the leg. The included angle γ is the angle θ between the head and the back.

2.4.2 Data Classification

Mark each frame of pictures with the following 5 poses:

The first category: lying on the left

The second category: lying on the right

The third category: bent legs

The fourth category: raising back

The fifth category: lying flat

The final database obtained by Kinect sensor is composed of 51762 frames of pictures, of which 10829 frames belong to the first category, 9944 frames belong to the second category, 10329 frames belong to the third category, 10333 frames belong to the fourth category, and 10327 frames belong to the fifth category.

Recognition is based on the selected angle features, where the left side is recognized by the angle μ, the right side is recognized by the angle α, the bent leg is recognized by the angle β, the back is recognized by the angle γ, and the lying down is recognized by the angle θ.

2.4.3 Neural Networks

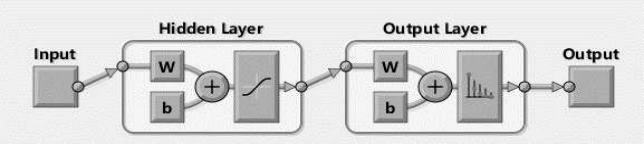

Fig. 8 Neural network structure diagram

The pose classification problem can be regarded as a static mapping problem, and the pattern recognition toolbox in the Matlab neural network toolbox can be used to realize the network required by the experiment in this paper. The Matlab pattern recognition toolbox is a two-layer feedforward network with a sigmoid hidden layer and softmax output neurons. As long as there are enough neurons in its hidden layer, the vector can be classified well. The network will be trained using the proportional conjugate gradient backpropagation algorithm, and the training function is trainscg. It is found through experiments that when the number of neurons in the hidden layer is

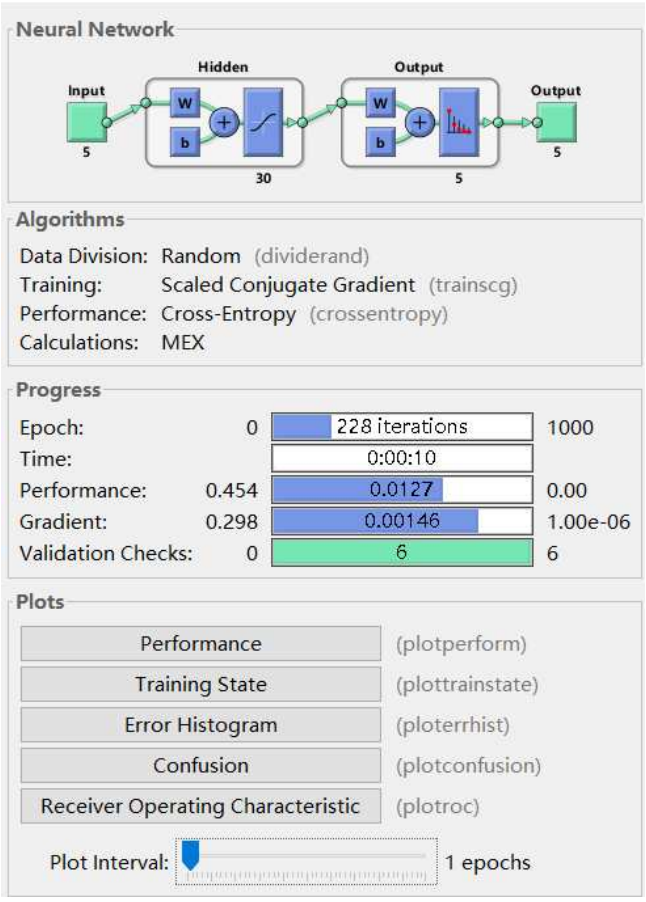

Fig. 9 Training process diagram

30, the experimental results are more accurate, and the training time is shorter, which only takes 10 seconds, as shown in Figure 9. Therefore, 30 neurons are set in the hidden

layer, which are connected to 5 input features. In the training process, the data set is classified, of which 70% is the training set, 15% is the validation set, and 15% is the test set.

3 Discussion and experimental results

When observing the experimental results, the accuracy of the experiment can be observed through the ROC curve and the confusion matrix.

Through the ROC curve, it is easy to find out a classifier's ability to recognize samples at a certain threshold. The best diagnostic limit value of a certain diagnostic method can be selected with the help of ROC curve. The closer the ROC curve is to the upper left corner, the higher the FPR and the lower the FPR of the test, that is, the higher.

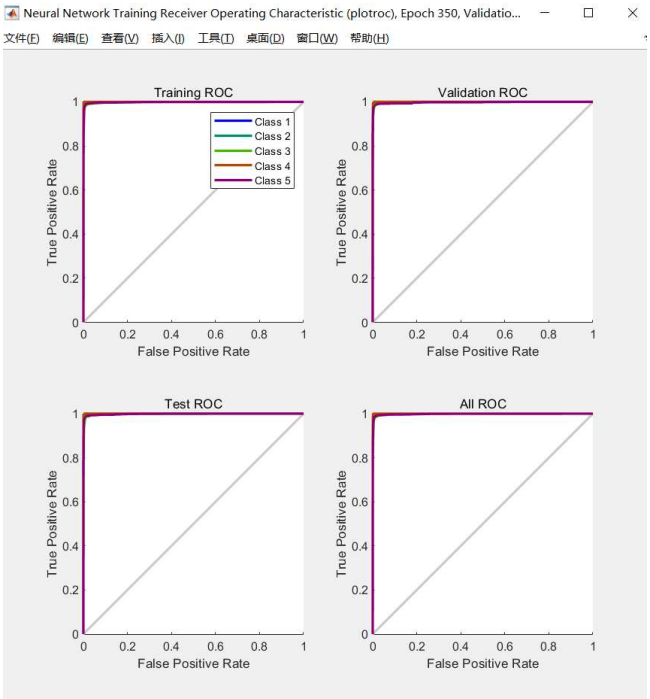

Fig.10 ROC curve

the sensitivity and the lower the false positive rate, the better the performance of the diagnostic method.

As shown in Figure 10 and Figure 11, the ROC curve obtained from the experiment shows that the ROC curves of the five types of postures are very close to the upper left corner, and it can be judged that the model adopted in this experiment has good performance. In addition, the confusion matrix can also be used to analyze the experimental results in more detail.

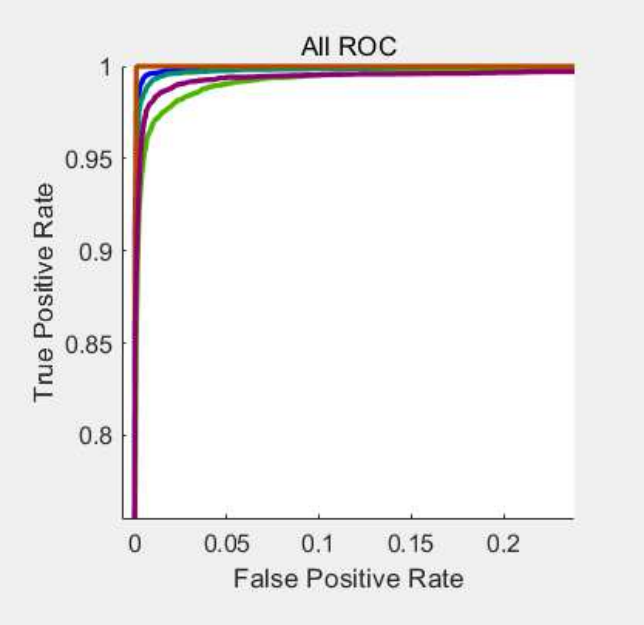

Fig.11 Partial enlarged view of ROC curve

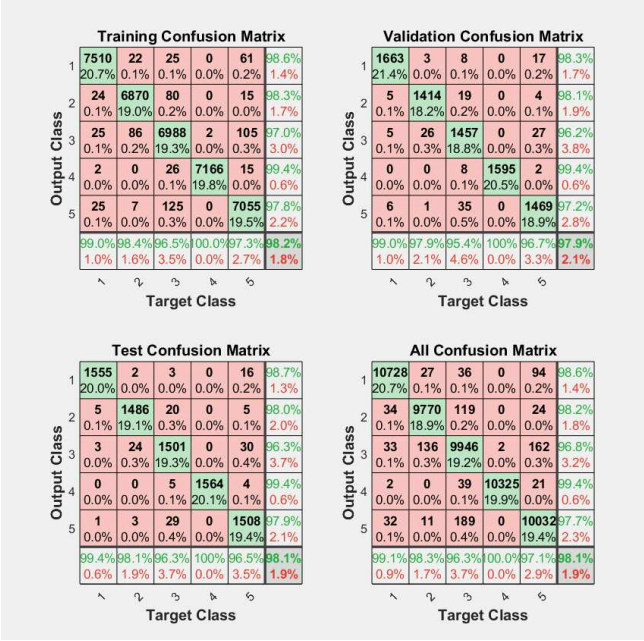

Fig.12 Confusion matrix result graph

Confusion matrix is the most basic, most intuitive, and easiest method to measure the accuracy of sub-type models. Through the confusion matrix, the accuracy of each classified data set and the average accuracy of all data can be seen, and the prediction. accuracy of the whole model can be judged by the accuracy.

As shown in Figure 12, the confusion matrix obtained from the experiment shows that the prediction model proposed in this experiment has achieved good results, with an overall average accuracy of 98.1%, among which the recognition efficiency of back lifting is the best, and the recognition accuracy is close to 100%. For the other four types of postures, there are two reasonable reasons at least that can be considered as the cause of the misclassification. First, the Kinect sensor acquires the bone coordinate points of the lying posture, as opposed to sitting and standing postures. Large error, some joint points need Kinect sensor system to reconstruct the joint posture, which will make the obtained result data relatively noisy, thereby affecting the accuracy of recognition. The second reason for the classification error may be that although careful principle features are used as a powerful description of body posture and are independent of the physical features of the subjects participating in the study, some similar postures will also have a greater impact on the experimental results. For the bending of the legs, the left side and the right side, when lying on the side, the degree of bending of the legs of a person will have a greater impact on the prediction results. When lying flat, the angle characteristics of the head and shoulders will also affect the recognition of the left and right side lying.

4 Conclusion

According to the results of this experiment, the human bone data preprocessing algorithm designed in this paper and the posture recognition model network obtained by the Matlab pattern recognition toolbox have good performance, with a recognition success rate of 98.1%, which is effective for the five postures of the human body. The distinction is more precise, which can make the intelligent care bed more intelligent and convenient, and greatly improve the safety and reliability of the intelligent care bed.

List of abbreviations：

Not applicable

Declarations：

Availability of data and materials:

Please contact author for data requests.

Competing interests:

The authors declare that they have no competing interests.

Funding:

This project received great support from the Changchun University of Science and Technology.

Authors' contributions:

XYM and QW conceived and designed the experiments. QW performed the experiments.CL, HSL and XQY participated in the acquisition of experimental data. QW wrote the paper. All authors took part in the discussion of the work described in this paper. All authors read and approved the final manuscript.

Acknowledgements:

The authors feel like showing the sincerest as well as grandest gratitude to the Changchun University of Science and Technology.

Authors' information:

Xianyu Meng: College of Mechanical and Electrical Engineering, Changchun University of Science and Technology, Weixing Road No.7089, Changchun, Jilin, China.

Qi Wang: College of Mechanical and Electrical Engineering, Changchun University of Science and Technology, Weixing Road No.7089, Changchun, Jilin, China.

References

[1] D. Pagliari, P. Livio, 'Calibration of Kinect for Xbox One and Comparison between the Two Generations of Microsoft Sensors'[J]. Sensors, 15(11) 11: 27569-27589 (2015)

[2] Q.Q. Wu, G.H. Xu, S.C. Zhang, Y. Li, F. Wei,in 42nd Annual International Conferences of the IEEE Engineering in Medicine and Biology Society, IEEE 'Human 3D pose estimation in a lying posture by RGB-D images for medical diagnosis and rehabilitation'[J]. 2020 : 5802-5805 (2020)

[3] B. Li, C. Han, B.X. Bai, 'Hybrid approach for human posture recognition using anthropometry and BP neural network based on Kinect V2'[J]. EURASIP Journal on Image and Video Processing, 2019(1) : 1-15.

[4] J. Maindonald, 'Pattern Recognition and Machine Learning'[J]. Journal of Statistical Software, 17(1) : 1-3 (2006)

[5] X. Chu, W. Ouyang, H. Li, X. Wang, in Conference on Computer Vision and Pattern Recognition. IEEE 'Structured feature learning for pose estimation' (2016), pp. 4715–4723

[6] W.J. Wang, J.W. Chang, S.F. Haung, 'Human posture recognition based on images captured by the Kinect sensor'[J].

International Journal of Advanced Robotic Systems, 13(2) : 29-36 (2016)

[7] A. Corti, S. Giancola, G. Mainetti, R. Sala, 'A metrological characterization of the Kinect V2 time-of-flight camera'[J]. Robotics and Autonomous Systems, 75 : 584-594 (2016)

[8] S.C. Hsu, J.Y. Huang, W.C. Kao, 'Human body motion parameters capturing using Kinect'[J].Machine Vision and Applications, 26(7-8) : 919-932 (2015)

[9] Y. Li, Z.J. Chu, Y.Z. Xin, 'Posture Recognition Technology Based on Kinect'[J]. IEICE Transactions on Information and Systems, E103.D(3) : 621-630 (2020)

[10] P.K. Pisharady, 'Kinect based body posture detection and recognition system'. Singapore (2013).

[11] H.Y. Shen, Determining the number of BP neural network hidden layer units. Tianjin Universitv Technology 5, 13 –15 (2008)

[12] C. Youness, M. Abdelhak, in 2016 13th International Conference on Computer Graphics, Imaging and Visualization (CGiV). IEEE. 'Machine learning for real time poses classification using Kinect skeleton data' (2016).

[13] X. Yang, Y. Tian, 'Effective 3D action recognition using Eigen Joints'[J]. Journal of Visual Communication and Image Representation (2014).

[14] R. A. Clark, Y. Pua, K. Fortin, C. Ritchie, 'Validity of the Microsoft Kinect for assessment of postural control'[J]. Gait & Posture, 36(3) : 372-377 (2012)

[15] Han, Artificial Neural Network Tutorial, 1st Ed (Beijing University of Posts and Telecommunications Press, Beijing), (2006)

[16] X. D. Li, Y. L. Wang, Y. He, G.Q. Zhu, 'Research on the algorithm of human single joint point repair based on Kinect'[J].Tech. Autom. Appl. 35(4), 96 –98(2016).

[17] L. Xia, C.C. Chen, J.K. Aggarwal, in Computer Vision and Pattern Recognition Workshops. IEEE.'Human detection using depth information by Kinect' (2011).

[18] R. Stefano, B. Giorgio, S. Micaela. 'Automatic Pose Recognition for Monitoring Dangerous Situations in Ambient-Assisted Living'[J]. Frontiers in bioengineering and biotechnology, 8 : 415 (2020)

Figures

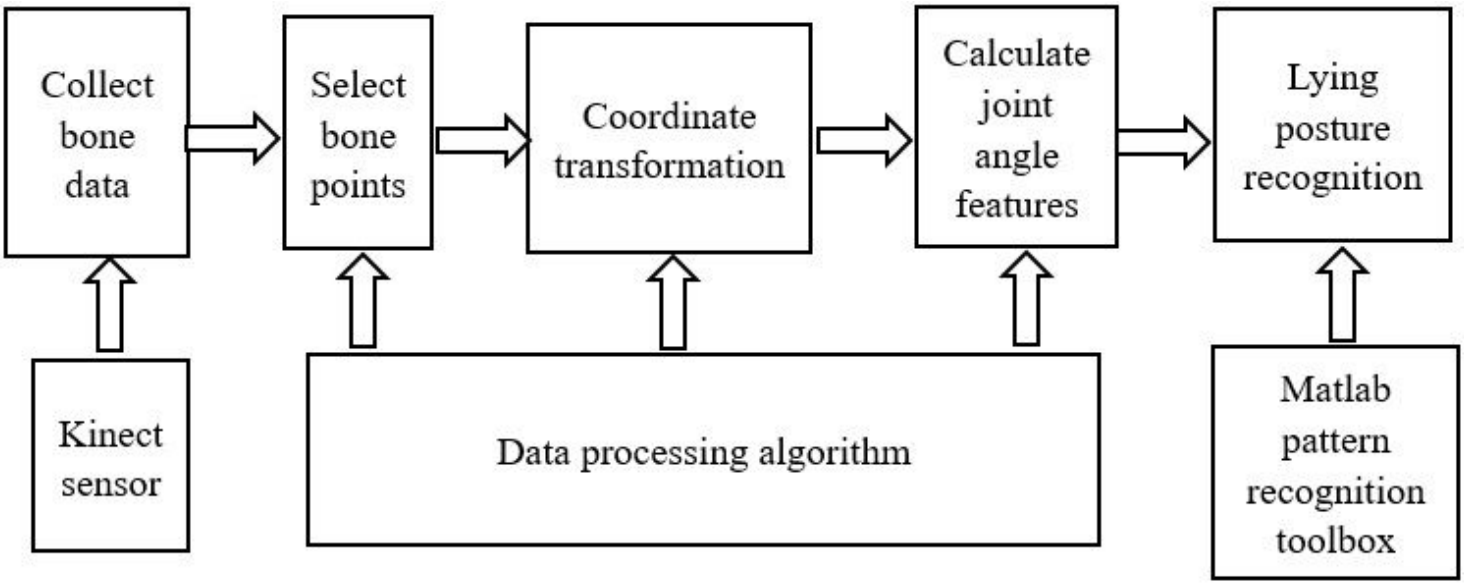

Figure 1

Model design flow chart

Figure 2

Human posture diagram

	x	y	z	x	y	z	x	y	z	x	y	z
Head	0.360343	0.433998	2.03399	0.362751	0.438181	2.03631	0.375324	0.448888	2.04386	0.375152	0.447817	2.04321
SpineShoulder	0.408351	0.285034	2.12404	0.409023	0.286061	2.1257	0.412423	0.288695	2.12954	0.411965	0.287238	2.1291
ShoulderLeft	0.26719	0.286823	2.24062	0.267294	0.293513	2.24344	0.268019	0.303929	2.25353	0.266748	0.302422	2.25196
ShoulderRight	0.531666	0.254488	2.07156	0.531742	0.251968	2.07092	0.534492	0.252397	2.07339	0.53488	0.253005	2.07396
SpineBase	0.385986	-0.13314	2.27621	0.395351	-0.13387	2.28492	0.384778	-0.1446	2.27178	0.378263	-0.1425	2.26378
HipLeft	0.448764	-0.13404	2.21755	0.458683	-0.13517	2.22209	0.439829	-0.15056	2.19987	0.433281	-0.14674	2.19249
HipRight	0.312565	-0.12885	2.27255	0.321977	-0.12869	2.2859	0.320698	-0.13466	2.28333	0.312511	-0.13522	2.27294
KneeLeft	0.174688	-0.21039	1.88368	0.185871	-0.20948	1.88677	0.252897	-0.19627	1.92797	0.218786	-0.18767	1.94277
KneeRight	-0.03258	-0.1958	2.01741	-0.00913	-0.20472	2.01403	0.011935	-0.14156	2.03395	0.057487	-0.1647	2.06951
AnkleLeft	0.019755	-0.43802	1.76122	0.002133	-0.40481	1.74806	0.052066	-0.39997	1.75648	0.063298	-0.38166	1.76744
AnkleRight	-0.10248	-0.40862	1.63718	-0.08301	-0.41396	1.66578	-0.06052	-0.37796	1.70966	-0.03659	-0.37032	1.7301

Figure 3

Part of the collected data diagram

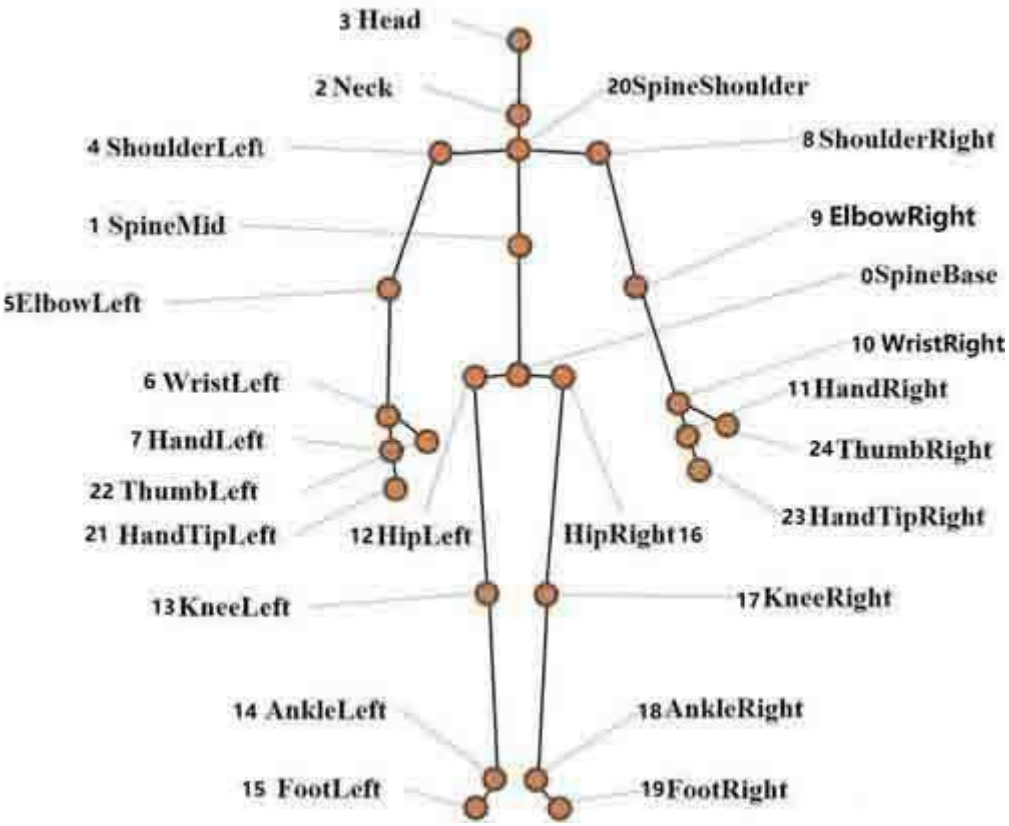

Figure 4

25 standardized bone joint points

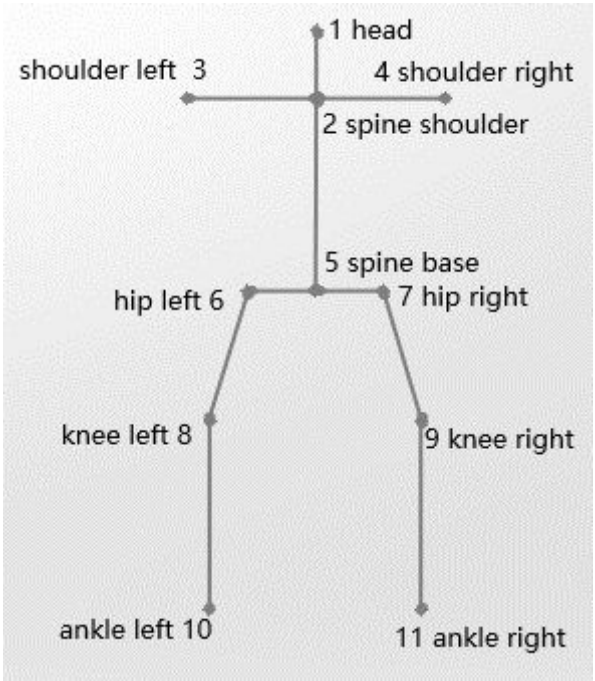

Figure 5

Coordinate diagram of 11 joint points

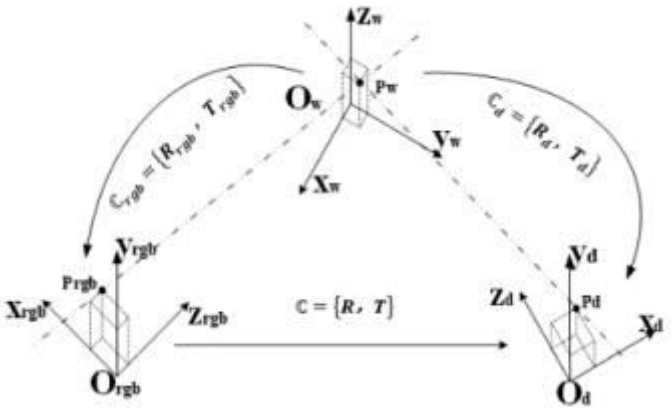

Figure 6

Coordinate transformation model

μ	α	β	γ	θ
90.02884	89.99931	91.37304	91.3349	90.35371
90.03275	89.98498	91.19414	91.79894	90.62031
90.03145	89.98374	91.25881	91.89519	90.60405
90.04135	89.9832	92.07469	91.25659	90.69108
90.04859	89.98171	91.7779	91.0944	90.69484
90.05041	89.98083	92.08256	92.56391	90.73667
90.05569	89.98037	91.9911	92.45289	90.74591
90.06052	89.98106	91.60578	91.9221	90.64708
90.06151	89.98185	91.17971	91.73123	90.61282
90.05996	89.9825	91.2544	91.94039	90.64067
90.05952	89.98235	91.27599	91.84926	90.63621
90.05818	89.98243	92.34753	91.96662	90.65368
90.05593	89.98263	92.48034	92.0082	90.62893
90.05602	89.98227	91.46762	92.24388	90.66315
90.05542	89.98271	91.33095	92.14475	90.64034
90.05567	89.98229	91.44611	92.3503	90.68249
90.05532	89.9819	92.1076	92.2835	90.6965
90.0545	89.98232	92.13376	92.43178	90.67318
90.05333	89.98237	92.18066	92.38876	90.6884
90.05278	89.98222	91.51078	92.7565	90.72148
90.05156	89.98221	91.46533	92.29784	90.67186
90.0514	89.98242	91.65727	92.20098	90.65457
90.05165	89.98277	91.53299	92.35413	90.66154
90.05296	89.98244	91.71136	92.50062	90.69881
90.05258	89.9829	91.55824	92.08239	90.64056
90.05273	89.98312	91.57112	92.15915	90.64271
90.05204	89.9832	91.33385	92.30261	90.65634
90.05158	89.98291	91.69997	92.38731	90.65542
90.05046	89.98501	91.43953	92.23699	90.69738

Figure 7

Partial angle feature data map

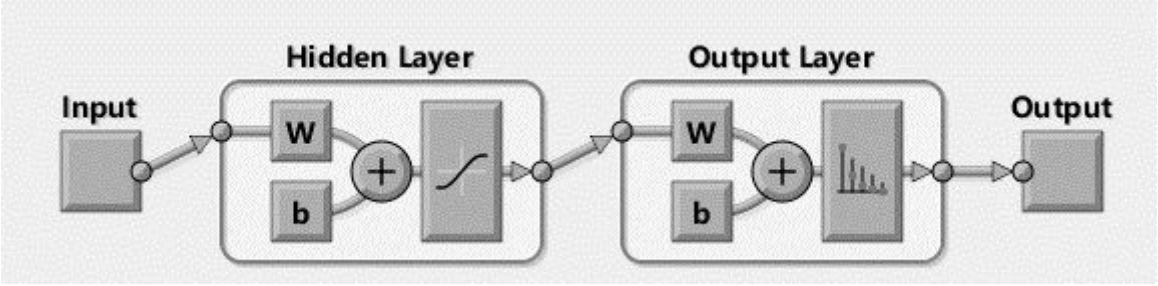

Figure 8

Neural network structure diagram

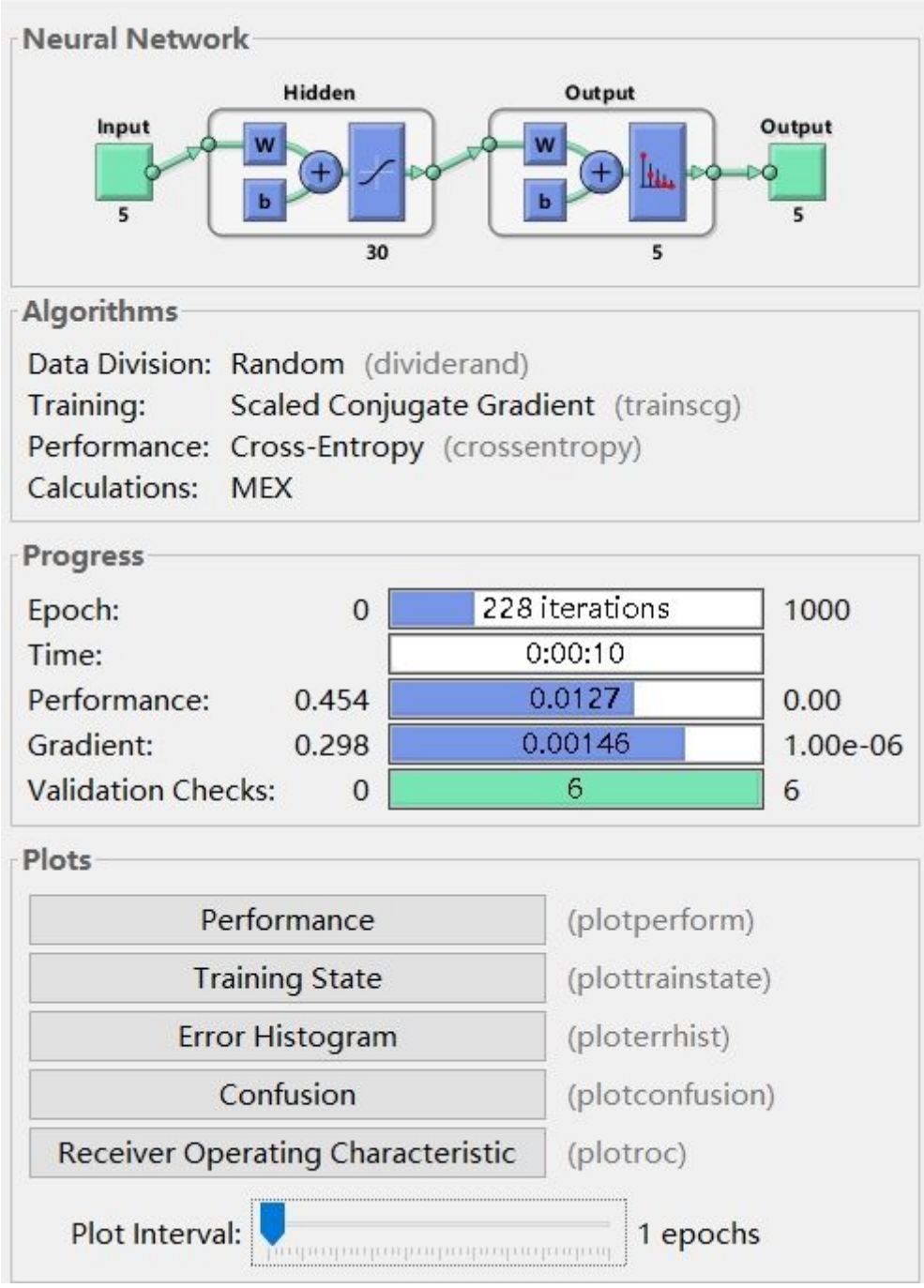

Figure 9

Training process diagram

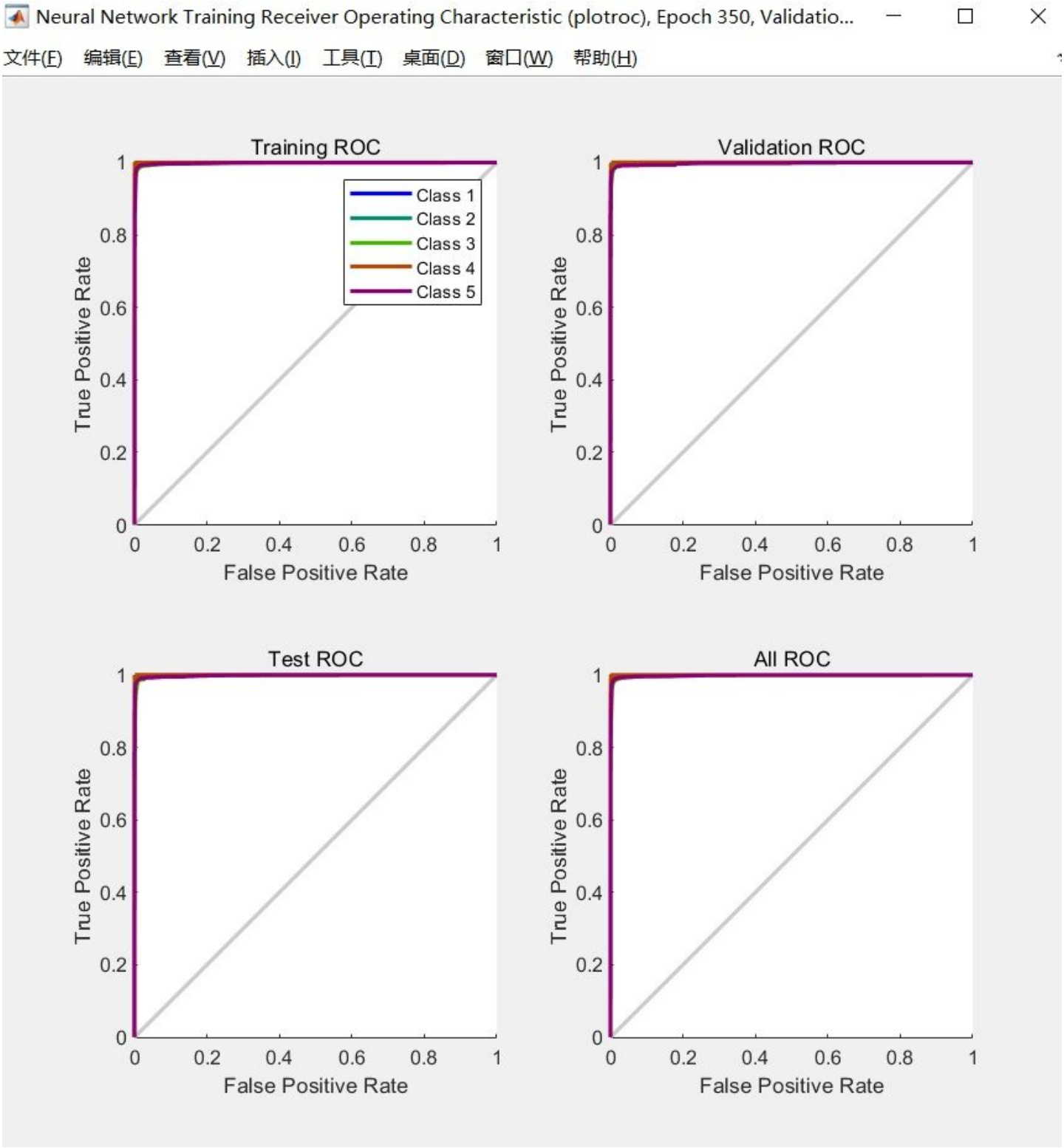

Figure 10

ROC curve

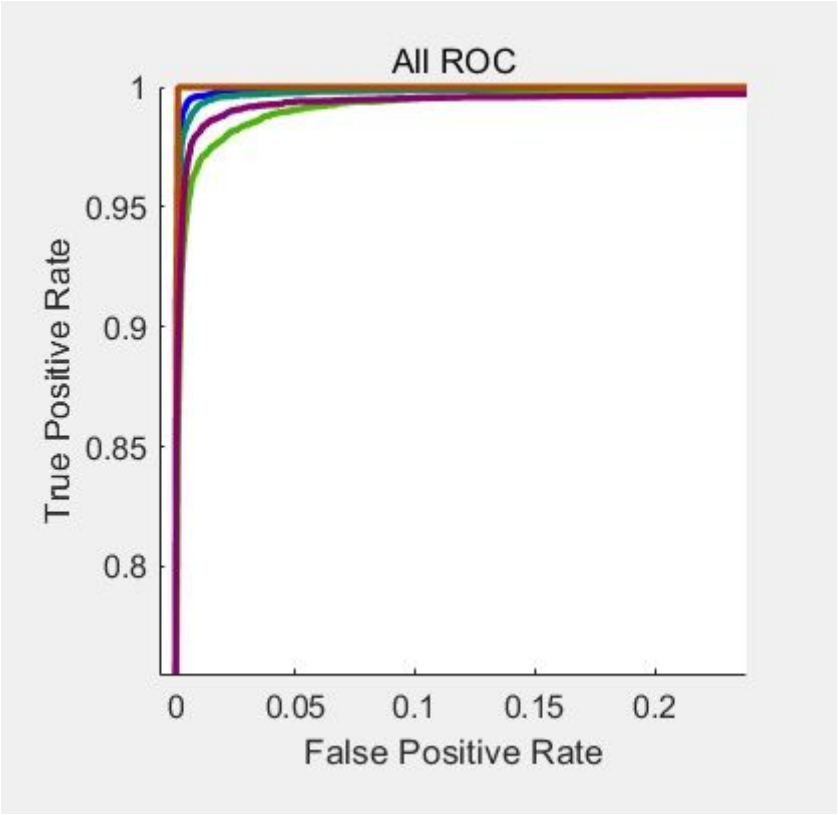

Figure 11

Partial enlarged view of ROC curve

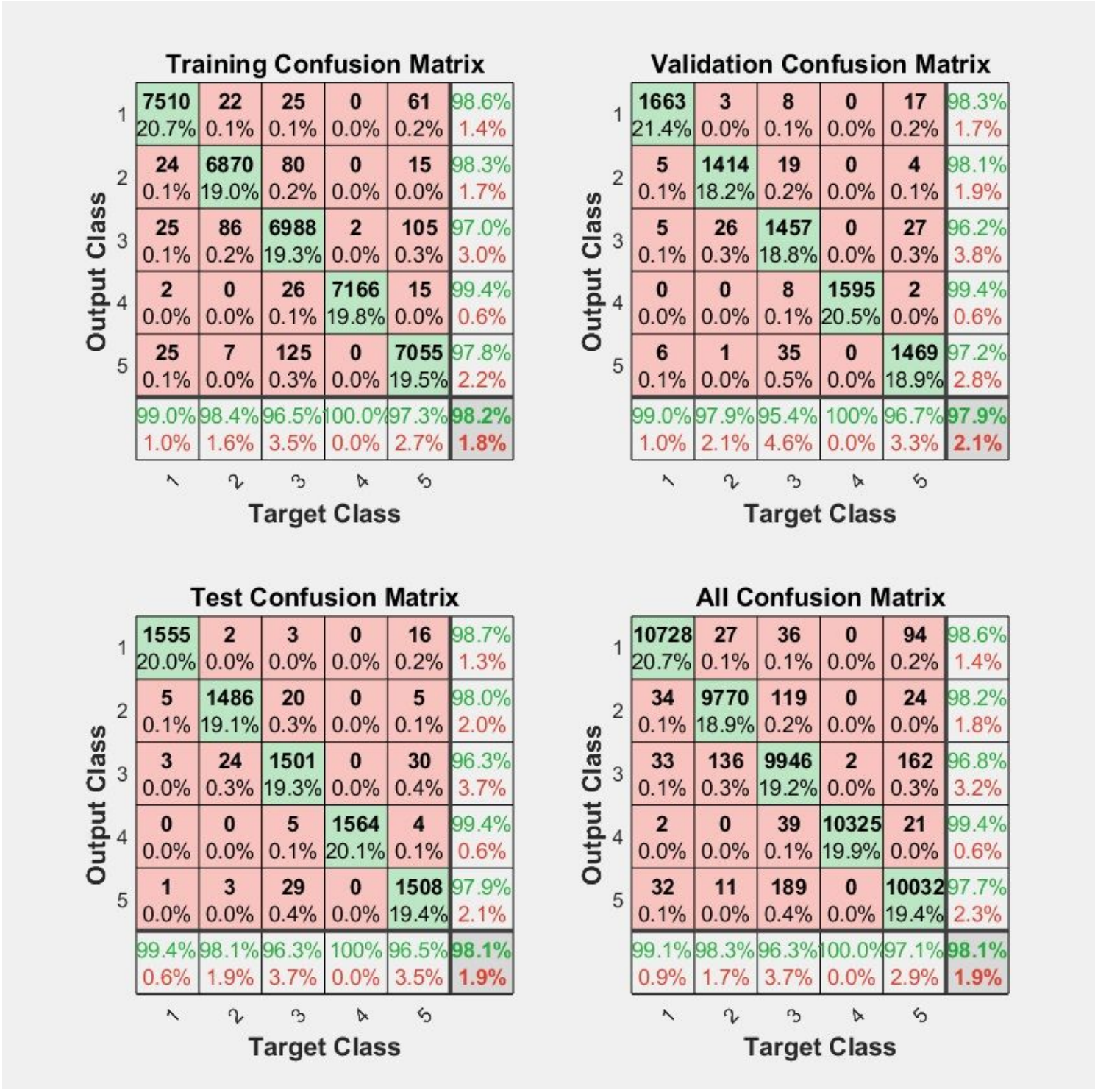

Figure 12

Confusion matrix result graph